Journal of Applied Polymer Science

Processing-Induced Degradation of Nanoclay Organic Modifier in Melt-Mixed PET/PE Blends During Twin Screw Extrusion at Industrial Scale: Effect on Morphology and Mechanical Behavior

Mohamed Yousfi,[1] Sophie Lepretre,[1] Jeremie Soulestin,[1] Bruno Vergnes,[2] Marie-France Lacrampe,[1] P. Krawczak[1]

[1]Department of Polymers and Composites Technology & Mechanical Engineering, MINES Douai, 941 Rue Charles Bourseul, CS 10838, 59508 Douai Cedex, France

[2]MINES ParisTech, CEMEF, UMR CNRS 7635, BP 207, 06904 Sophia-Antipolis Cedex, France

Correspondence to: J. Soulestin (E-mail: jeremie.soulestin@mines-douai.fr)

ABSTRACT: Immiscible PET/PE blends (80/20 wt %) were prepared on an industrial twin-screw extruder with and without different types of commercially available montmorillonites (Cloisite® C15A, C10A, and 30B), containing organic surfactants differing by their polarities and their thermal stability). XRD and TEM observations evidence an intercalated structure, C15A leading to a better dispersion compared to C30B and C10A. The size of the PE dispersed phase decreases upon addition of organoclays (OMMT), suggesting an efficient compatibilization. The most efficient compatibilizing effect is observed in the case of C15A (smallest droplet size and narrowest size distribution). Nevertheless, elongation at break in tension and impact strength of PET/PE blends drastically decrease upon addition of OMMT, whatever the organoclay added, due to a possible degradation of the clay surfactant during melt compounding, which counteracts the nanofiller compatibilization effect. Furthermore, similar PET/PE/OMMT blends prepared at a lab scale using a microcompounder are ductile contrary to those compounded in the industrial extruder, which show a brittle behavior. This difference was ascribed to the extrusion residence time (much higher in an industrial extruder than in a lab micro-compounder), which appeared to be a key parameter in controlling the clay surfactant degradation and thus the end-use properties of such immiscible blends. © 2013 Wiley Periodicals, Inc. J. Appl. Polym. Sci. **2014**, *131*, 39712.

KEYWORDS: blends; clay; compatibilization; morphology; mechanical properties

Received 2 April 2013; accepted 27 June 2013

DOI: 10.1002/app.39712

INTRODUCTION

Compatibilization of immiscible polymers is an efficient way to obtain new materials that combine the desirable properties of more than one polymer. The compatibilizer is usually either a copolymer containing functional groups able to react with one or two polymer phases of the blend.[1–5] Another compatibilization alternative has recently emerged. It consists in adding nanofillers (clay,[6–10] carbon nanotubes,[11–13] and silica[14]) to improve the interfacial interactions between the polymer blend components. In that case, the nanofillers are expected to play the role of both structural reinforcement and compatibilizer. The addition of solid particles also results in an increase of polymer melt viscosity, which further helps reducing the size of the dispersed polymer phase.[6] The processing conditions (type of extruder, shear rate, residence time…) also play an important role in controlling the final properties of polymer blends.[15]

For the past 10 years, increasing research efforts have been focused on compatibilization of melt-mixed polymer blends by organoclays, generally organo-modified montmorillonite (OMMT). Aiming at identifying the mechanisms involved in compatibilization, many authors have examined the evolution of polymer blends morphology upon addition of clay. In the case of PS/PMMA blends compatibilized by OMMT, Gelfer et al.[16] reported a decrease in PS droplet size attributed to the compatibilizing effect of the clay surfactant and to higher viscosity. Meanwhile, Wang et al.[17] explained the significant decrease of the PS domain size in PS/PP blends in presence of clay by the presence of PS and PP chains between the clay layers, thus forming block copolymers. Voulgaris and Petridis[18] investigated the effect of modified clay (hectorite-DMDO) on PS/PEMA blend with PEMA as matrix. The authors claimed that clay adsorbs PEMA chains and creates PEMA/hectorite-intercalated DMDO structures, in which PS chains form separate domains of decreasing size as the clay concentration increases.

Attention has also been drawn on the localization of nanoclay, either at polymer blend interface or within the polymer phase

Table I. Organoclays Modifier Specifications

OMMT commercial name	Cloisite© 10A	Cloisite© 15A	Cloisite© 30B
Modifier chemical name	2MBHT	2M2HT	MHT2EOH
Modifier chemical structure	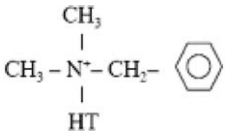	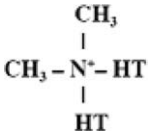	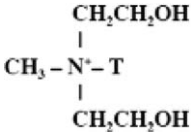
Anion	Chloride	Chloride	Chloride
Modifier concentration (wt %)	39	43	30
Basal spacing (nm)	1.92	3.15	1.85

of preferred affinity. In the case of PP/PET/OMMT (Cloisite© 10A) blends compatibilized by PP-g-MA, Calcagno et al.[19] reported that the clay was localized preferentially at the interface of PP/PET and in PET phase, because of the higher compatibility of the clay used with polymers containing polar groups. Hong et al.[20] highlighted the role of modified clay having affinities with PBT on the morphology of immiscible PBT/PE blends. Adding a small amount of clay led to a sharp decrease in the size of the dispersed phase. When added at very small amount, the clay was localized at the interface whereas, at higher amount, it was found preferentially in the phase with which it has the greatest affinity (PBT).

Furthermore, the issue of the relationship existing between the induced morphology and the resulting mechanical performance has been addressed. The homogeneity of the blend morphology and the quality of the nodule/matrix interface appear to strongly influence the mechanical properties of the compounded material. Ray et al.[8] showed that an organoclay (Cloisite© 20A) added to PS/PP blends acts as both a filler and a compatibilizer. It was localized preferentially at the interface and significantly reduced the interfacial tension and the size of the dispersed polymer phase. The maximum tensile stress of PS/PP blends decreased upon addition of clay, whereas in contrast the elongation at break increased, confirming a better adhesion between the phases in presence of clay. Kusmono et al.[21] showed that the addition of clay (montmorillonite-octadecylamine) to a PP/PA6 blend led to an increase of the blend stiffness, an increase of its maximum tensile stress due to the reinforcing effect of clay and a decrease of its elongation at break ascribed to the chain mobility restriction induced by the exfoliation of platelets. In addition, the impact properties of the blend decreased in presence of clay. Calcagno et al.[19] observed that the addition of clay to PP/PET blend led to poor mechanical properties (tensile yield stress, elongation at break and impact strength), which was attributed to poor dispersion of clay (presence of tactoids). Also, Wang et al.[22] highlighted two opposing effects of clay in the case of PA6/EPDM-g-MA/clay blends. On one hand, clay had a negative effect on the interfacial adhesion because of its shield effect on the interactions between maleic anhydride and PA6. On the other hand, it prevented the coalescence of nodules of EPDM-g-MA, inducing a decrease of EPDM-g-MA droplet size. Due to poor interfacial adhesion, the addition of clay tended to reduce the impact properties of the blend, even-though the stiffness and maximum tensile stress increased. This brief review of several results published in the literature evidences that the influence of organoclay on mechanical properties is complex and strongly depends on the studied blend systems.

In a previously published work, using different commercial OMMT (Cloisite© C10A, C15A and C30B), we showed that the morphology of PET/PE blends compatibilized by OMMT was controlled by the clay organo-modifier (surfactant) itself and not by the presence of montmorillonite platelets.[4] Also, the final morphological and mechanical properties of PET/PE blends appeared to strongly depend on the thermal stability of the clay surfactant.[5] A tailor-made phosphonium organo-modified clay was found to be the most efficient, compared to other less thermally stable commercial OMMT (such as Cloisite© 10A and 30B). In these studies, the PET/PE/organoclay compounds were prepared using a micro-compounder (i.e. at moderate shear rate and short residence time) which cannot reflect industrial manufacturing conditions.

The present article aims at evaluating the efficiency of clay organic modifier as compatibilizing agent of immiscible PET/PE polymer blends, compounded in real industrial conditions (high shear rate and long residence time in an industrial twin-screw extruder). The induced morphology and resulting mechanical properties in tension and under impact of the compounded nanocomposites will be characterized. The importance of the thermal stability and processing-induced degradation of clay organo-modifier will also be pointed out based on a comparison of the results achieved in industrial scale and lab scale compounding conditions.

EXPERIMENTAL

Materials

Low density polyethylene (PE) (Riblene FF 20, density 0.921 g/cm^3, melt flow index 0.8 g/10 min [190°C, 2.16 kg], melting temperature 112°C) was supplied by Polimeri Europa (Italy). Poly(ethylene terephtalate) (PET) pellets (density 1.4 g/cm^3, intrinsic viscosity 0.98 dL/g at 30°C, melting temperature 250°C) were supplied by Acordis (The Netherlands). The clays provided by Southern Clay Products (USA) are sodium montmorillonite substituted with quaternary ammonium chloride,

respectively modified by 2MBHT (dimethyl, benzyl, hydrogenated tallow) for Cloisite® 10A (C10A), 2M2HT (dimethyl, dehydrogenated tallow) for Cloisite® 15A (C15A) and MHT2EOH (methyl, tallow, bis-2-hydroxyethyl) for Cloisite® 30B (C30B) (Table I). Hydrogenated tallow (HT) is made of around 65% C18, 30% C16, and 5% C14. The surfactants of C30B, C15A, and C10A have a special affinity with PET, polyolefins, and both PET and polyolefins, respectively.

Samples Preparation

Before extrusion, PET pellets were dried in a vacuum oven overnight at 120°C. PET/PE (80/20 wt %) and PET/PE/OMMT (80/18/2 wt %) or (80/16/4 wt %) blends were prepared using an industrial co-rotating twin-screw extruder (Clextral BC 45, France), having a 50 mm screw diameter and a $L/D = 24$ length/diameter ratio. Blends of each composition were compounded under the same mixing conditions. The barrel temperature settings ranged from 240 to 270°C. The screw rotational speed was set-up at 77 rpm which corresponds to a residence time of about 6 min. The extrudate was then cooled in water and pelletized.

Some compounds were also prepared at 270°C using a conical co-rotating twin-screw micro-compounder (Minilab, Rheomex CTW5, Germany), having a 10 mm average diameter. The screw rotational speed was set-up at 50 rpm which corresponds to a residence time of about 1 min. Using the recirculation mode of the apparatus, it was possible to change the mixing time (1 or 6 min) while keeping the same shear rate.

The shear rate in the extruders was calculated using eq. (1)[15]:

$$\dot{\gamma} = \frac{\pi \times D \times N}{60 \times h}. \quad (1)$$

where D is the screw diameter, N the rotational screw speed and h the gap between the screw and the barrel. Its average value is 40 s^{-1} in the case of the industrial extruder and 50 s^{-1} in the case of the micro-compounder.

Standard test samples for mechanical testing were molded using an electric injection-molding machine (KM 80–160E, Krauss-Maffei, Germany).

For XRD characterization, disks of 25-mm diameter and 1-mm thickness were cut out of 115 × 115 × 2 mm^3 test plates previously compression-moulded by hot pressing (Dolouets 383, France) at a temperature of 270°C and under a pressure of 11 MPa applied during 5 min.

Characterization

Blends morphology was examined by scanning electron microscopy on an instrument (SEM, Hitachi S4300 SE/N, Japan) operating at accelerating voltage of 15 kV and a probe current of 130 pA. SEM photographs of the PET/PE and PET/PE/OMMT blends were taken from injection-molded samples fractured in liquid nitrogen and then coated with gold to avoid charging on the fracture surface. The average PE domain diameters and their distribution were measured on the fractured surfaces by means of an image analysis software (ImageJ©). A minimum of 210 particles were analyzed for each composition. TEM observations were performed on a transmission electron microscope (Philips CM12, Netherlands) operating at an accelerating voltage of 120 kV. The TEM samples, around 90-nm thick, were cut at −80°C

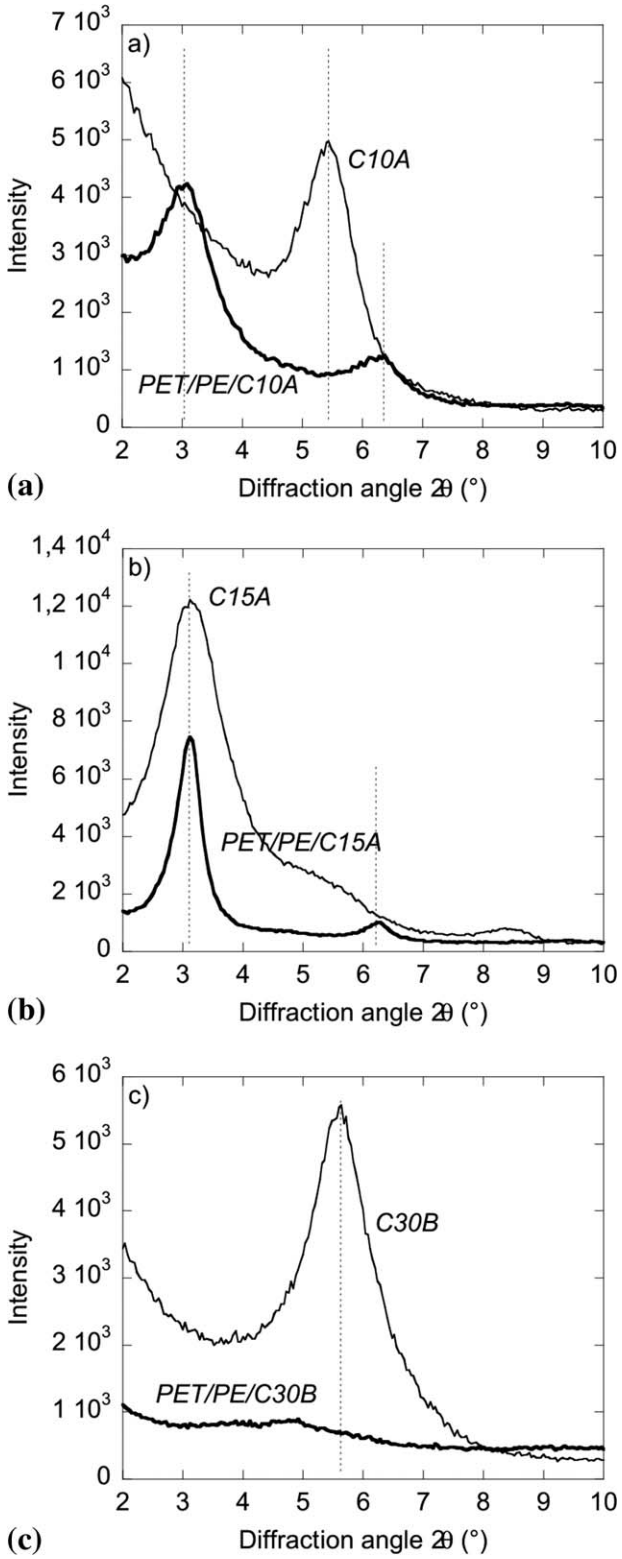

Figure 1. XRD patterns for the OMMT and the PET/PE/OMMT (80/18/2 wt %) blends prepared in an industrial extruder—(a) C10A, (b) C15A, (c) C30B.

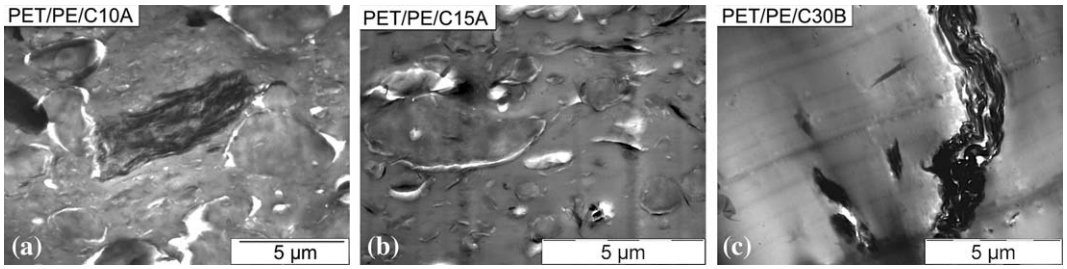

Figure 2. TEM micrographs of the PET/PE (PET/PE= 80/20) and PET/PE/OMMT (PET/PE/OMMT = 80/18/2 wt %) blends prepared in an industrial extruder.

from the injection-molded samples by using an ultracryomicrotom (Ultracut, Leica Microsystems, Germany) equipped with 2 mm Cryo diamond knives (Diatome, Switzerland).

XRD curves were recorded on a horizontal diffractometer (D8 Bruker, Germany) operating at 40 kV and 40 mA with a beam consisting of CoKα radiation ($\lambda = 1.78897$ Å). Data were collected in the 2θ region 2–10°, with a step size of 0.004° and a counting time of 30 s per step. The basal spacing of the organically modified layered silicate before and after intercalation was estimated from the position of (d_{001}) peak in the XRD diffractogram according to the Bragg equation ($\lambda = 2d \sin \theta$), where d is the spacing between silica layers of the clay, λ the X-ray wavelength and θ the reflection angle on the silica layer.

Tensile tests were carried out at 23 ± 2°C and 50 ± 5% relative humidity on a standard tensile machine (Model 5585H, Instron) at a cross-head speed of 1 mm min^{-1} (for modulus measurement) or 10 mm min^{-1} (for ultimate properties measurement) according to ISO 527. The mechanical properties (Young modulus, tensile strength and elongation at break) were determined from the recorded load-displacement curves. Charpy impact tests were carried out using a 15 J pendulum (Model 5101, Zwick, Germany) on both notched and unnotched samples according to ISO 179-1. All the reported values were calculated as averages over five specimens at least for each compound composition.

RESULTS AND DISCUSSION

Structure and Morphology Analysis

Interlayer Spacing in OMMT and PET/PE/OMMT Blends. The space gallery was determined using the Bragg law for the OMMT and the PET/PE/OMMT blends elaborated using the industrial extruder. A decrease in the degree of coherent layer stacking (i.e., a more disordered system) of the clay would lead

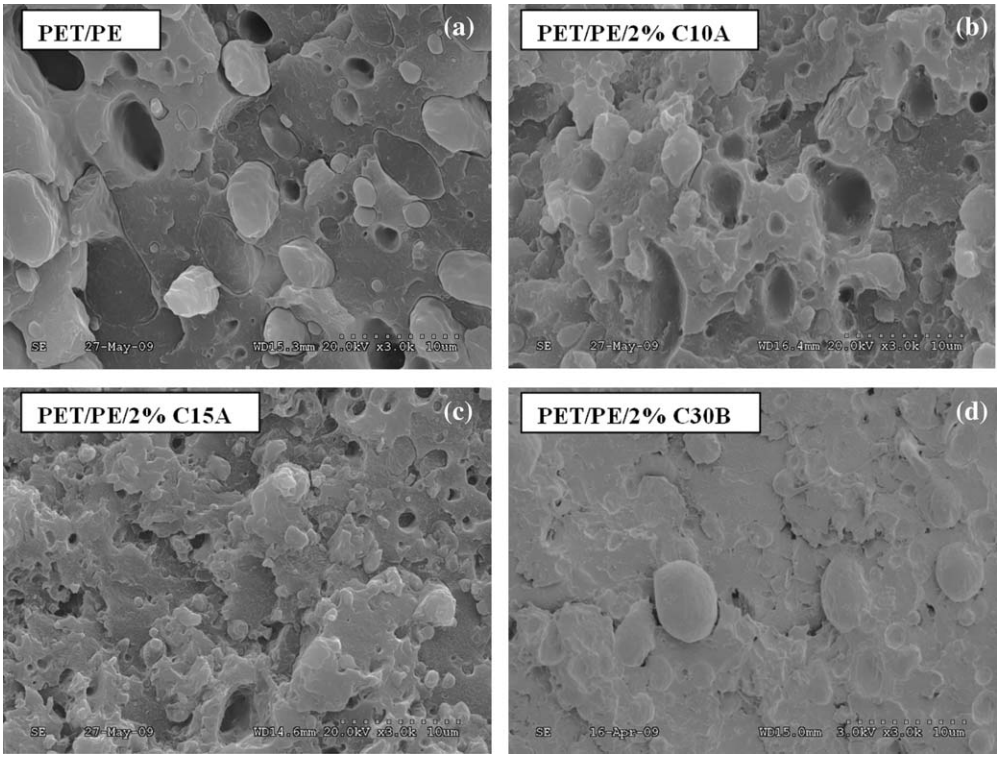

Figure 3. SEM micrographs of fracture surfaces of the PET/PE (PET/PE= 80/20) and PET/PE/OMMT (PET/PE/OMMT = 80/18/2 wt %) blends prepared in an industrial extruder.

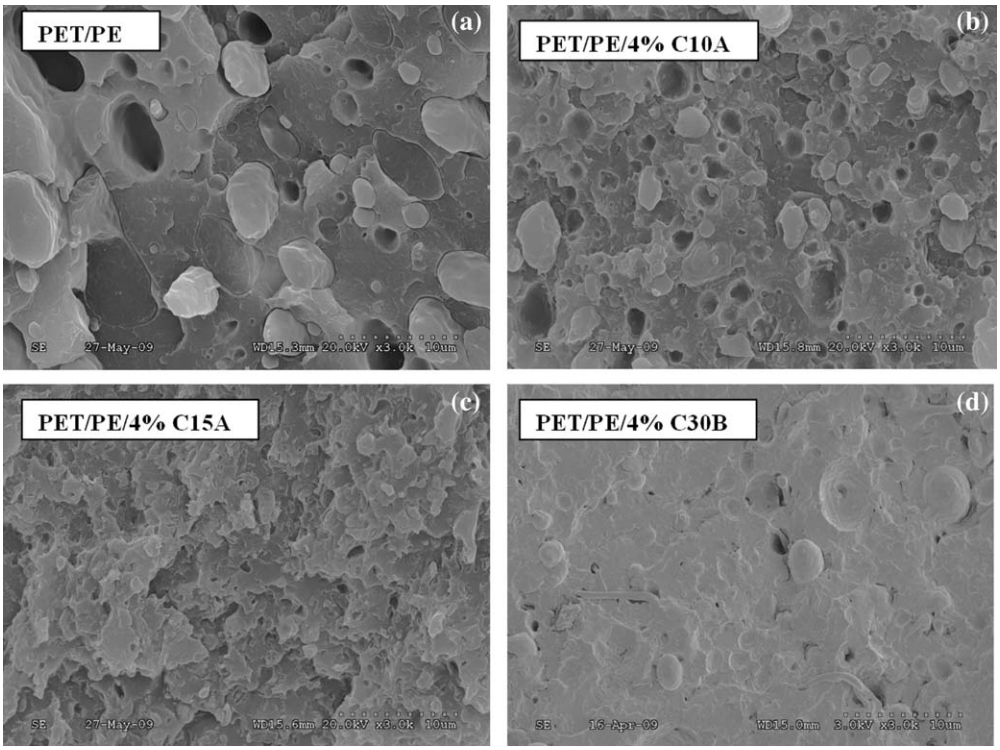

Figure 4. SEM micrographs of fracture surfaces of the PET/PE (PET/PE = 80/20) and PET/PE/OMMT (PET/PE/OMMT = 80/16/4 wt %) blends prepared in an industrial extruder.

to a peak broadening and an intensity decrease in the XRD diffractogram. Figure 1 shows the XRD patterns of neat C10A, C15A, C30B organoclays, and PET/PE/OMMT blends. The primary (d_{001}) diffraction peaks of neat C10A, C15A, and C30B are located around $2\theta = 5.4°$, 3.13°, and 5.62°, respectively, which gives interlayer spacing (d-spacing) of 1.89, 3.27, and 1.82 nm, respectively. These values are very close to the data provided by Southern Clay Products (Table I).

When C10A clays was added to the PET/PE blend, XRD peak was shifted to lower angles indicating an increase in interlayer spacing due to polymer intercalation. The average distance between the platelets is then about 3.31 nm instead of 1.89 nm before intercalation. In the case of the PET/PE/C15A blend, no peak displacement is observed. A narrowing of the characteristic clay peak is noticed but this does not prove that intercalation has not occurred. Because of the wide galleries of C15A ($d = 3.27$ nm), PET could intercalate and substitute the surfactant in the interlayer region without increase of the basal spacing. In the case of the PET/PE/C30B blend, the absence of signal in the XRD pattern may indicate a partial exfoliation even if not necessarily a complete exfoliation of clay. Indeed, since the clay percentage is low, the sensitivity of WAXD and the relatively weak diffraction intensity probably lead to an undetectable signal.

To confirm these results, TEM observations were carried out on the blends containing C10A, C15A, and C30B organoclays (Figure 2). In the case of C10A and C30B [Figure 2(a,c)], intercalated structures are observed with the presence of many clay aggregates. On the contrary in the case of C15A [Figure 2(b)], clay platelets are better dispersed even if clay tactoids are still visible and despite few exfoliation only. This result may be surprising as C30B has a solubility parameter which is the closest to the PET matrix one and which theoretically should induce a better dispersion of clay in PET/PE blends.[10]

Morphology of PET/PE and PET/PE/OMMT Blends. Figures 3 and 4 show the cryofractured surfaces of PET/PE blends containing 2 and 4 wt % of organo-modified nanoclay, respectively, compounded using the industrial extruder. In absence of nanoclay, the two-phase morphology and a large PE droplet size (diameter $D = 4.2$ μm in average) are typical of poor interfacial bonding.

The blends morphology significantly changes upon addition of nanoclay. The PE domain dimensions are remarkably reduced and more evenly dispersed, leading to a more homogeneous structure in terms of polydispersity of the nodule sizes. Such a morphology modification indicates that the compatibility of PET and PE is greatly improved in presence of OMMT, which seems to avoid the coalescence between the PE domains; consequently, the PE droplets are smaller and uniformly distributed. The addition of 2 wt % of organoclay decreases the PE droplet size by 40% at least and up to 80% [Figure 5(a)]. The addition of higher amounts of OMMT (e.g., 4 wt %) amplifies this trend [Figure 5(b)]. Moreover, the droplets size distribution is narrowed by the addition of OMMT, particularly of C15A (Figure 6).

Among the three OMMT used in the present work, C15A made it possible to achieve the highest decrease of the PE droplet size ($D = 1.56$ μm in average for 2 wt % clay), whereas C30B was

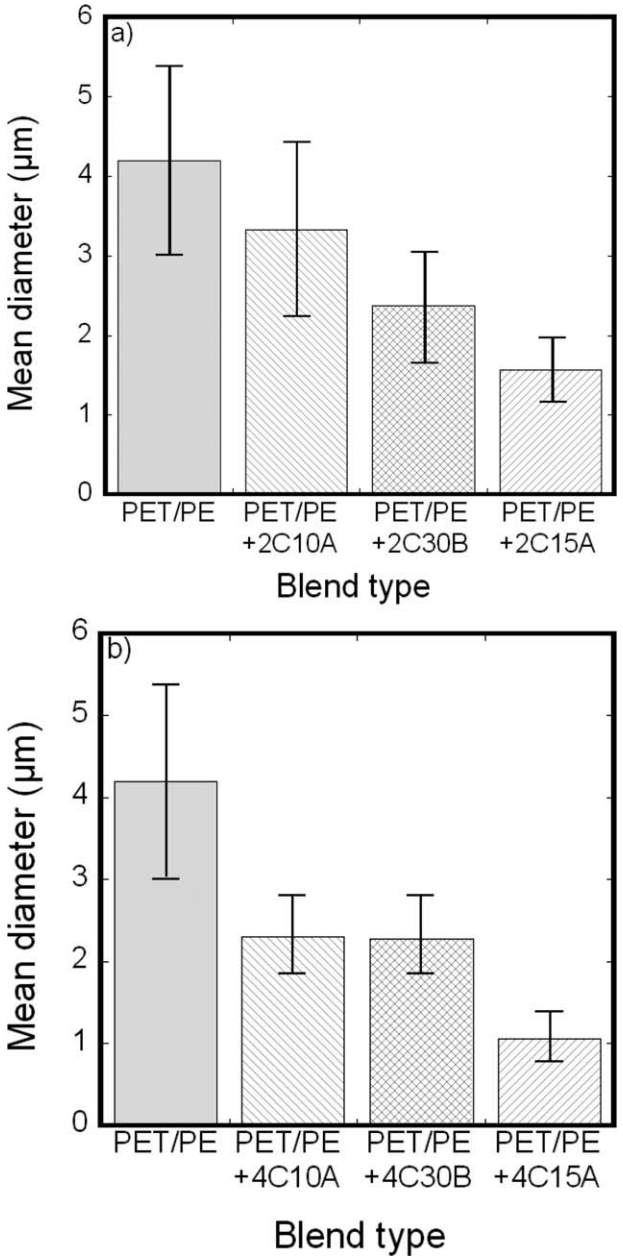

Figure 5. Average PE droplets diameter for the different blends prepared in an industrial extruder - (a) PET/PE/OMMT = 80/18/2 wt %; (b) PET/PE/OMMT = 80/16/4 wt %.

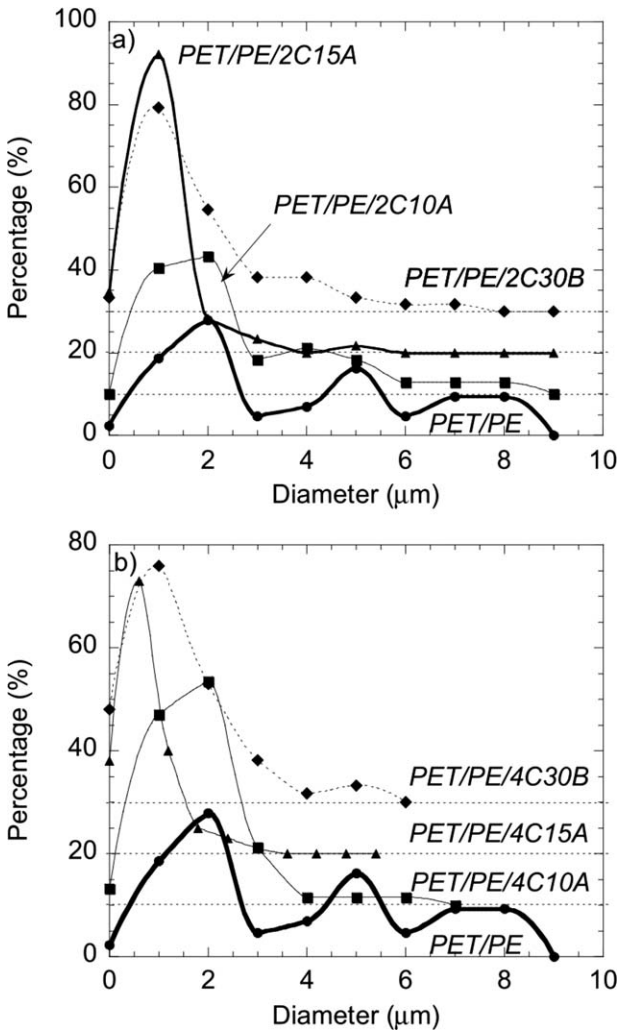

Figure 6. Particle size distribution for the different blends prepared in an industrial extruder - (a) PET/PE/OMMT = 80/18/2 wt %; (b) PET/PE/OMMT = 80/16/4 wt %. Curves have been vertically shifted by respectively 10, 20, and 30%, in order to be distinguished more easily.

less efficient ($D = 2.4$ μm in average for 2 wt % clay) and C10A led to the smallest decrease ($D = 3.3$ μm in average for 2 wt % clay and 2.4 μm in average for 4 wt % clay) and the larger polydispersity of PE dispersed phase.

The explanation of the PE droplet size decrease upon clay addition may be based on the model developed by Serpe et al.[23] [eq. (2)], which states the existence of a relationship between the diameter (D) of the droplet of dispersed phase, the interfacial tension (Γ) between the two polymer components at a temperature equal to the mixing temperature, the shear rate ($\dot{\gamma}$), the viscosity ratio between the dispersed phase (η_{PE}) and the blend (η_{blend}) viscosities, and the volume fractions of each phase (Φ_{PE} and Φ_{PET}).

$$D \approx \frac{\left[\frac{4\Gamma}{\dot{\gamma}\times\eta_{blend}}\left(\frac{\eta_{PE}}{\eta_{blend}}\right)^{a}\right]}{1-\left(4\Phi_{PE}\,\Phi_{PET}\right)^{0.84}}. \quad (2)$$

α is an experimental parameter, with a value of nearly 0.84, which is positive if the viscosity ratio is larger than one. This relationship shows that, although the interfacial tension has a great influence on the droplet size, the viscosity ratio is also important in the case of a PET/PE/OMMT systems. Increasing the OMMT content from zero up to 2 wt % and then 4 wt % increases the blend viscosity and therefore reduces the mean PE droplet size much more. Comparable results were observed by other authors in similar blend systems.[21,24]

Based on the TEM images (Figure 2) and whatever the type of the organoclay used, it seems that the fillers are localized in

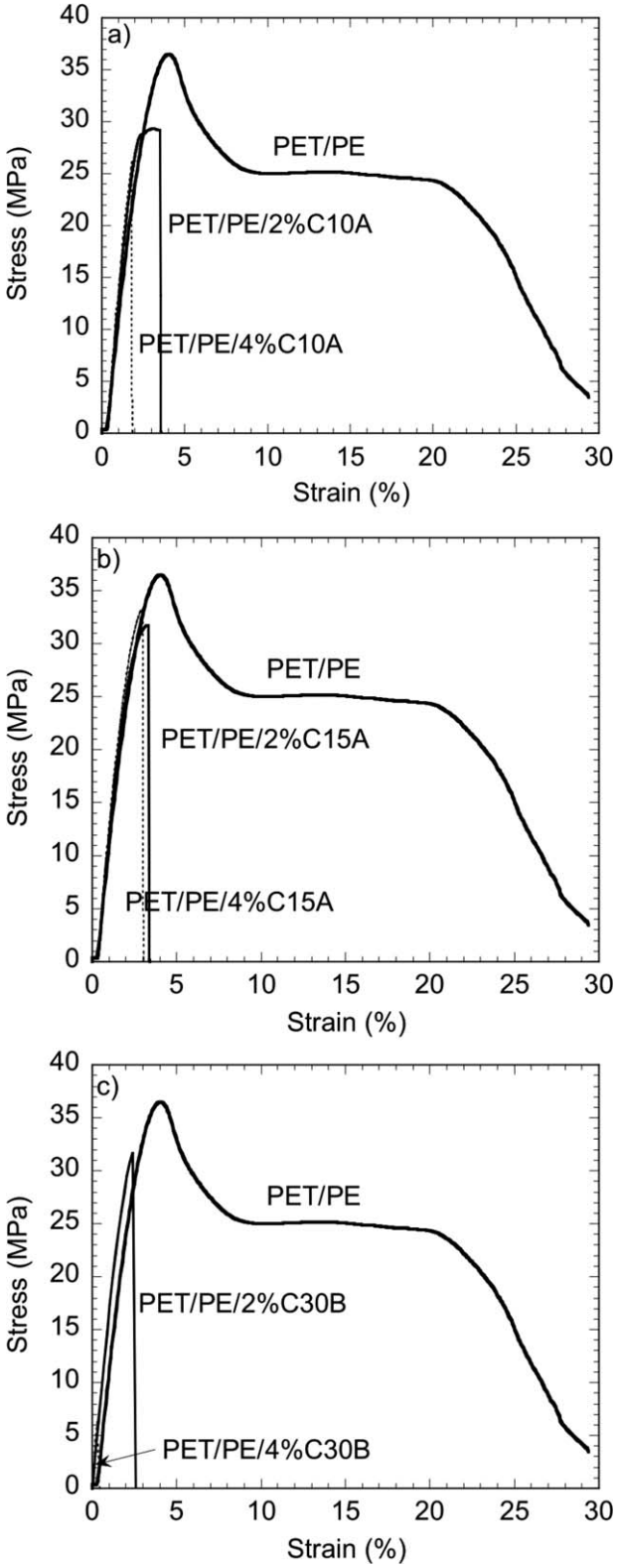

Figure 7. Stress–strain tensile curves for PET/PE and PET/PE/ OMMT blends prepared in an industrial extruder at different clay concentrations (2 and 4 wt %). a) C10A, b) C15A, c) C30B.

PET matrix as well as in LDPE dispersed phase domains. Few particles were localized at the interface. More precisely, in the case of C10A filled PET/PE systems; the majority of these nanoparticles are localized inside PET matrix. Some nanoparticles are also evident at the interface, even though a discontinuous coverage of LDPE nodules was observed exhibiting a stack defect structure.[6,7] The mean thickness of stacks calculated was 62 ± 41 nm. In the case of PET/PE/C15A blends, we observe a competition between a local and a stack defect around the PE minor phases. The mean thickness of stacks was 42 ± 20 nm. For C30B filled PET/PE composites, very few particles exist at the interface, the majority of these particles are localized in PET matrix in the form of large aggregates with a mean thickness of 106 ± 52 nm.

It is worth noting that although the PET/PE/OMMT blends were prepared in an industrial extruder with a quite long residence time (6 min), the decreasing trend observed for the PE droplet size is the same as the one previously noticed at lab scale using a micro-compounder and fully different processing conditions (shear rate of 50 s^{-1} and a residence time of 1 min).[4,5] Interestingly, an industrial scale-up does not change the positive effect of organoclay addition on the blends morphology.

Mechanical Behavior

Tensile Properties. Figure 7 and Table II show the tensile behavior and properties of neat PET/PE and PET/PE/OMMT blends prepared using the industrial extruder. Whatever the clay type and concentration, the Young modulus significantly increases upon addition of organoclay, the highest values being obtained with C10A, whereas the maximum stress and the elongation at break (ε_R) decrease. The PET/PE blend is ductile ($\varepsilon_R = 20$–30%) whereas PET/PE/OMMT blends are frankly brittle ($\varepsilon_R < 4\%$), despite the aforementioned improvement of their morphologies.

Such a trade-off of mechanical properties was often reported in the case of PET/OMMT nanocomposites.[25] Wang et al.[26] observed that the elongation at break and the impact resistance of PET decreased with increasing concentration of modified montmorillonite, whereas the maximum stress and the Young modulus sharply increased. Similarly, Kráčalík et al.[27] studied the effect of the addition of C10A and C30B on the mechanical and rheological properties of recycled PET. Although the Young modulus increased and the filler was well dispersed in the PET matrix, a clear decrease of the tensile strength and elongation at break (from 316.5% for neat PET down to 5.1 and 19.2% in presence of 5 wt % of C10A and C30B, respectively) was noticed by these authors upon addition of OMMT. The authors explained these results as a consequence of the thermal degradation of the clay surfactant modifier (degradation temperature = 180°C) during the extrusion process at 270°C. Indeed, the degradation products of quaternary ammonium at high temperature also results in a decrease of the mechanical performance of PET matrix.[5] For this reason, using more thermally stable imidazolium[28–30] or phosphonium[31] salts instead of quaternary ammonium salts is sometimes preferred.

Actually, we have previously shown and reported in another paper[5] for similar PET/PE/OMMT blends prepared with a lab

Table II. Tensile Mechanical Properties of PET/PE and PET/PE/OMMT Blends Prepared in an Industrial Extruder at Different Clay Concentrations (2 and 4 wt %)

Material	Young modulus (MPa)	Yield stress (ductile behavior) (MPa)	Stress at break (brittle behavior) (MPa)	Elongation at break (%)
PET/PE	1615 ± 21	36.3 ± 0,5	-	24.2 ± 0.3
PET/PE + 2 wt % C10A	2089 ± 16	-	30.0 ± 2.1	2.8 ± 0.6
PET/PE + 2 wt % C15A	1770 ± 62	-	31.5 ± 1.0	2.9 ± 0.4
PET/PE + 2 wt % C30B	1800 ± 46	-	23.7 ± 11.4	1.6 ± 1.0
PET/PE + 4 wt % C10A	2088 ± 19	-	24.3 ± 1.8	1.7 ± 0.1
PET/PE + 4 wt % C15A	2035 ± 17	-	32.9 ± 0.4	2.8 ± 0.1
PET/PE + 4 wt % C30B	1777 ± 43	-	6.9 ± 0.9	0.3 ± 0.1

micro-compounder that the set-up processing temperature (270°C) is well above the onset temperature of degradation of the organoclay (decomposition of C10A, C15A, and C30B starts at 180, 238, and 230°C, respectively). For all the organoclays used, the extent of mass loss increases as a function of time, and more and more degradation products from the clay surfactant are produced in these conditions. These degradation products attack mainly the PET matrix via chemical mechanisms and subsequently induce the brittleness of the PET/PE/OMMT blends; this effect should be enhanced when the residence time of the polymer blend in the extruder increases. Despite this problem, it was nevertheless possible to retain the blend ductility ($\varepsilon_R = 40\%$) at least for C30B, which is obviously not the case here when the compounds are prepared with an industrial twin-screw extruder. As mentioned in "Morphology of PET/PE and PET/PE/OMMT Blends" Section, it is worth noting that the PET/PE/ OMMT blends compounded with the industrial extruder sustained a quite long residence time (6 min, i.e., six times longer than the mixing time used in the lab micro-compounder).

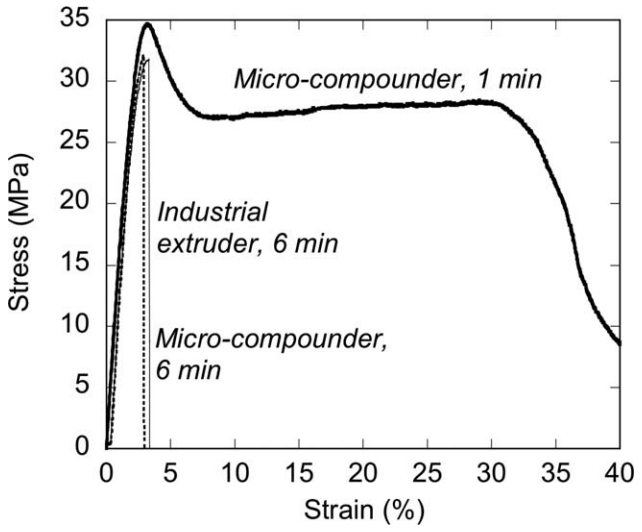

Figure 8. Stress-strain tensile curves of PET/PE/2 wt % C15A blends prepared in a twin-screw extruder (industrial scale, residence time 6 min) and a micro-compounder (lab scale, residence times 1 and 6 min).

To highlight the suspected effect of the extrusion residence time on the mechanical properties of PET/PE/ OMMT blends, the tensile behavior of the PET/PE/2 wt % C15A blend compounded in the industrial extruder (residence time $t = 6$ min) was compared to that of the counterpart blend prepared in the lab micro-compounder, alternatively with short ($t = 1$ min) and long ($t = 6$ min) residence times. In the latter case, the recirculation mode of the micro-compounder was used to keep the shear rate constant while reaching the same residence time ($t = 6$ min) as that experienced by the blend prepared in the industrial extruder. The stress–strain tensile curves of the three compounds are shown in Figure 8. The blend prepared in the micro-compounder with a residence time of 1 min is ductile, whereas the one extruded with a residence time of 6 min is brittle and therefore behaves as the one prepared in the industrial extruder. This confirms that the ductility loss of PET/PE blends observed upon addition of organoclay is related to a too long residence time during extrusion. Thus, it seems difficult to use at industrial scale commercial organoclays having limited thermal stability as compatibilizers for immiscible polymer blends requiring high extrusion temperatures.

Impact Strength. Figure 9 shows both the notched and unnotched Charpy impact strengths of PET/PE blends, compounded using the industrial extruder, containing or not 2 and 4 wt % of OMMT. The impact strength of the PET/PE blend drastically decreases upon addition of clay, whatever the clay type and content, even though C15A has a less negative effect. Although C15A and C30B have almost similar onset temperatures of decomposition, C15A chemical structure is less sensitive to thermo-oxidation than that of C30B which contains hydroxides groups favorable for the formation of olefins and other products of degradation at high temperature.[32]

The results of mechanical testing show that the end-use performances (and particularly the ductility) of PET/PE/ OMMT blends are not only governed by their morphological structure, but also by a possible processing-induced degradation of the organic surfactant during melt-mixing. In that case, both the thermal stability (decomposition temperature) of the organomodifier and the residence time in the extruder are key influence parameters.

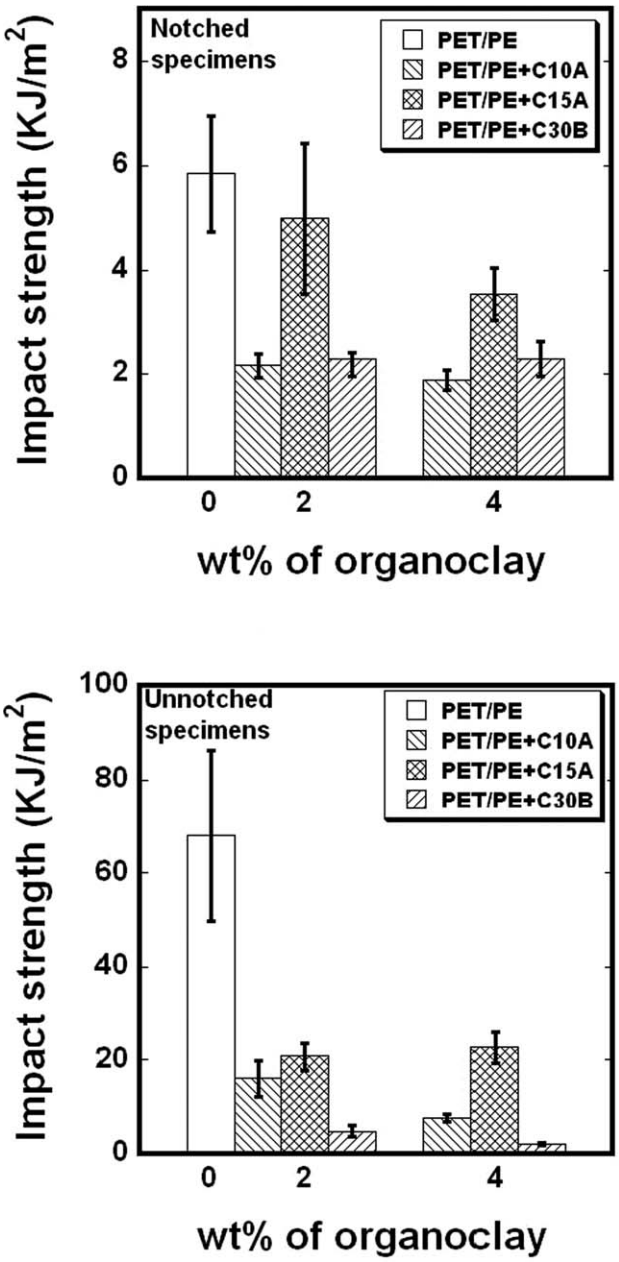

Figure 9. Notched (a) and unnotched (b) Charpy impact strength of PET/PE and PET/PE/OMMT blends prepared in an industrial extruder as a function of clay mass concentration.

CONCLUSIONS

The morphology and mechanical properties of immiscible PET/PE blend prepared on an industrial extruder and compatibilized with different organoclay were investigated as a function of the type of clay surfactant organo-modifier (Cloisite®, C10A, C30B, and C15A, differing by their affinities respectively with both PE and PET, PET, PE and by their increasing thermal stability). An improvement in the morphologies of PET/PE/OMMT blends is achieved after addition of organoclays, with better compatibilization efficiency in presence of C15A compared to C10A and C30B. Nevertheless, whatever the clay surfactant organo-modifier used, a brittle behavior of PET/PE/OMMT blends is observed compared to corresponding neat blends, which is suspected to be due to thermal degradation of the clay organomodifier during compounding. However, at a lab scale (micro-extruder), the mechanical properties of PET/PE/OMMT blends were found to be better (higher ductility) than those prepared at an industrial scale. This suggests that the extrusion residence time plays a major role in controlling the final morphology and the mechanical performance of immiscible polymer blends compatibilized by nanoclay. Thus, the end-use mechanical properties of such polymer blends appear to depend more on the degradation of clay organomodifiers than on the enthalpic interactions between the blend components and the surfactants used for the clay modification.

ACKNOWLEDGMENTS

This work was financially supported by the Carnot M.I.N.E.S Institute (France) in the frame of the "Nanostructure" project carried out by its NanoMines working group. The authors are indebted for valuable assistance provided by Damien Betrancourt and Laurent Charlet from Mines Douai in microscopy and extrusion experiments, respectively. The authors also gratefully acknowledge the International Campus on Safety and Intermodality in Transportation (CISIT), the Nord-Pas-de-Calais Region and the European Community (FEDER funds) for funding contribution to the micro-compounder and the scanning electron microscope.

REFERENCES

1. Kalfoglou, N.; Skafidas, D.; Kallitsis, J.; Lambert, J.; and Vanderstappen, L. *Polymer* **1995**, *36*, 4453.
2. Martínez, J. G.; Benavides, R.; and Guerrero, C. *J. Appl. Polym. Sci.* **2007**, *104*, 560.
3. Lee, J. H.; Ruegg, M. L.; Balsara, N. P.; Zhu, Y.; Gido, S. P.; Krishnamoorti, R.; and Kim, M.-H. *Macromolecules* **2003**, *36*, 6537.
4. Yousfi, M.; Soulestin, J.; Vergnes, B.; Lacrampe, M.-F.; Krawczak, P. *Macromol. Mater. Eng.*, **2013**, *298*, 757.
5. Yousfi, M.; Soulestin, J.; Vergnes, B.; Lacrampe, M.-F.; Krawczak, P. *J. Appl. Polym. Sci.* **2013**, *5*, 2766.
6. Huitric, J.; Ville, J.; Mederic, P.; Moan, M.; Aubry, T. *J. Rheol. 53*, 1101 **2009**.
7. Ville, J.; Mederic, P.; Huitric, J.; Aubry, T. *Polymer* **2012**, *53*, 1733.
8. Sinha Ray, S.; Pouliot, S.; Bousmina, M.; Utracki, L. A. *Polymer* **2004**, *45*, 8403.
9. Sinha Ray, S. and Bousmina, M. *Macromol. Rapid Commun.* **2005**, *26*, 450.
10. Sinha Ray, S. and Bousmina, M. *Macromol. Rapid Commun.* **2005**, *26*, 1639.
11. Baudouin, A.-C.; Bailly, C.; Devaux, J. *Polym. Degrad. Stab.* **2010**, *95*, 389.
12. Baudouin, A.-C.; Devaux, J.; Bailly, C. *Polymer* **2010**, *51*, 1341.
13. Baudouin, A.-C.; Auhl, D.; Tao, F.; Devaux, J.; Bailly, C. *Polymer* **2011**, *52*, 149.

14. Tong, W.; Huang, Y.; Liu, C.; Chen, X.; Yang, Q.; Li, G. *Colloid Polym. Sci.* **2010**, *288*, 753.
15. Maric, M. and Macosko, C. W. *Polym. Eng. Sci.* **2004**, *41*, 118.
16. Gelfer, M.; Song, H.; Liu, L.; Hsiao, B.; Chu, B.; Rafailovich, M.; Si, M.; Zaitsev, V. *J. Polym. Sci. Part B: Polym. Phys.* **2003**, *41*, 44.
17. Wang, Y.; Zhang, Q.; Fu, Q. *Macromol. Rapid Commun.* **2003**, *24*, 231.
18. Voulgaris, D. *Polymer* **2002**, *43*, 2213.
19. Calcagno, C.; Mariani, C.; Teixeira, S.; Maurer, R. *Compos. Sci. Technol.* **2008**, *68*, 2193.
20. Hong, J.; Namkung, H.; Ahn, K.; Lee, S.; Kim, C. *Polymer* **2006**, *47*, 3967.
21. Kusmono, Mohdishak, Z.; Chow, W.; Takeichi, T.; *Rochmadi Eur. Polym. J.* **2008**, *44*, 1023.
22. Wang, K.; Wang, C.; Li, J.; Su, J.; Zhang, Q.; Du, R.; Fu, Q. *Polymer* **2007**, *48*, 2144.
23. Serpe, G.; Jarrin, J.; Dawans, F. *Polym. Eng. Sci.* **1990**, *30*, 553.
24. Hong, J. S.; Kim, Y. K.; Ahn, K. H.; Lee, S. J.; Kim, C. *Rheol. Acta* **2006**, *46*, 469.
25. Kim, K. H.; Kim, K. H.; Huh, J.; Jo, W. H. *Macromol. Res.* **2007**, *15*, 178.
26. Wang, Y.; Gao, J.; Ma, Y.; Agarwal, U. *Compos. Part B: Eng.* **2006**, *37*, 399.
27. Kráčalík, M.; Studenovský, M.; Mikešová, J.; Kovářová, J.; Sikora, A.; Thomann, R.; Friedrich, C. *J. Appl. Polym. Sci.* **2007**, *106*, 2092.
28. Awad, W. H.; Gilman, J. W.; Nyden, M.; Davis, R. D.; Harris, R. H.; Sutto, T. E.; Callahan, J. H.; Delong, H. C.; Trulove, P. C. *Molten Salts XIII* **2002**, *200*, 2002.
29. Davis, C. H.; Mathias, L. J.; Gilman, J. W.; Schiraldi, D. A.; Shields, J. R.; Trulove, P.; Sutto, T. E.; Delong, H. C. *J. Polym. Sci. Part B: Polym. Phys.* **2002**, *40*, 2661.
30. Gilman, J. W.; Awad, W. H.; Davis, R. D.; Shields, J.; Harris, R. H.; Davis, C.; Morgan, A. B.; Sutto, T. E.; Callahan, J.; Trulove, P. C.; Delong, H. C. *Chem. Mater.* **2002**, *14*, 3776.
31. Costache, M. C.; Heidecker, M. J.; Manias, E.; Wilkie, C. A., *Polym. Adv. Technol.* **2006**, *17*, 764.
32. Cervantes-Uc, J.; Cauich-Rodriguez, J.; Vazquez-Torres, H.; Garfias Mesias, L.; Paul, D. *Thermochim. Acta* **2007**, *457*, 92.